Article

Tree species composition governs urban phenological responses to warming

Zhaofei Wu [1,2,10], Constantin M. Zohner [2,10], Yuyu Zhou [3], Thomas W. Crowther [2], Hongzhou Wang[4], Yiming Wang [5], Josep Peñuelas [6,7], Yufeng Gong[1], Jian Zhang [8], Yibiao Zou[2], Johan Van den Hoogen[2] & Yongshuo H. Fu [1,4,9] ✉

Urban environments are typically warmer than surrounding rural areas, providing a unique setting for studying phenological responses to climate warming. Phenological differences between urban and rural trees are driven by local climate and species composition. Yet, the extent to which species composition influences phenological responses to urbanization remains poorly understood. To address this, we combine manipulative experiments, satellite-derived phenology data, and georeferenced tree occurrence records. Our findings show that, across Northern Hemisphere cities, differences in the temperature sensitivity of spring phenology between urban and rural areas are largely driven by urban-rural variation in species composition, surpassing the effects of preseason temperature. This pattern is particularly pronounced in Asian cities, where urban areas exhibit 0.74 ± 0.24 days/°C higher temperature sensitivity than rural areas. In-depth analyses using experiments and high-resolution satellite imagery from Beijing further demonstrate species-specific phenological responses to urbanization, with urban-dominant species exhibiting higher temperature sensitivity in urban environments compared to rural ones. These findings show that both interspecific variation in temperature sensitivity and species-specific responses to urbanization contribute to the pronounced impact of species composition on urban-rural phenological patterns. Our study underscores the importance of considering species composition when studying phenological responses to climate warming, especially in urban contexts.

Human-induced climate change has caused changes in plant phenology[1–3], affecting the structure and function of terrestrial ecosystems[4–6]. In addition, the urban heat island effect has caused many urban areas to exhibit higher temperatures than adjacent rural regions[7,8].

These urbanized zones offer unique opportunities to study how ecosystems react to human disturbances and rising temperatures[9,10]. In recent years, urban tree phenology has received increasing attention due to its direct impact on water, energy and carbon fluxes, as well as its role

[1]College of Water Sciences, Beijing Normal University, Beijing 100875, China. [2]Institute of Integrative Biology, ETH Zurich (Swiss Federal Institute of Technology), Zurich, Switzerland. [3]Department of Geography and Institute for Climate and Carbon Neutrality, The University of Hong Kong, Hong Kong, China. [4]School of National Safety and Emergency Management, Beijing Normal University, Beijing 100875, China. [5]USDA-ARS Hydrology and Remote Sensing Laboratory, Beltsville, MD, USA. [6]CREAF, Cerdanyola del Vallès, Barcelona, Catalonia, Spain. [7]CSIC, Global Ecology Unit CREAF-CSIC-UAB, Bellaterra, Barcelona, Catalonia, Spain. [8]School of Life Sciences, Sun Yat-sen University, Guangzhou 510275, China. [9]Plants and Ecosystems, Department of Biology, University of Antwerp, Antwerp, Belgium. [10]These authors contributed equally: Zhaofei Wu, Constantin M. Zohner. ✉e-mail: yfu@bnu.edu.cn

in modifying the albedo effect[11–13]. Although the magnitude of urban temperature gradients is a key factor driving phenological differences between urban and rural areas, the composition of tree species–each with distinct responses to warming[5,11,14]–likely plays an equally important role. However, the relative influence of species composition and urban climate on phenological responses to urbanization remains poorly understood.

Given the large impact of temperature on plant physiology, it is key to understand how urbanization affects the temperature sensitivity of vegetation phenology. Recent satellite-derived data suggest that urban warming reduces the sensitivity of spring vegetation phenology to temperature[10], meaning that the start of season advances by fewer days per degree of warming in urban areas compared to rural ones. However, studies have so far provided mixed evidence for this[15,16], likely due to the substantial interspecific variation in phenological responses to temperature[1,11,14]. Urban-rural differences in species composition may therefore greatly impact the relationship between local temperatures and tree phenology.

Urban environments often host a wide range of species from diverse climatic and phylogenetic origins. Consequently, urban areas not only differ in species composition from their rural counterparts but also tend to exhibit higher species richness[17,18]. In natural forests, greater species richness has been shown to reduce phenological sensitivity to temperature, either directly through the presence of temperature-resilient species or indirectly via mechanisms such as deeper root systems and altered soil processes[19–21]. This raises an important question: do phenological differences between urban and rural areas primarily reflect variations in species identities, or are they driven by differences in species richness? Despite the importance of this question, interspecific variations in phenological sensitivity have not yet been thoroughly quantified in urban phenology studies[11,22,23].

In this study, we analyzed ground-sourced and satellite-derived data from 135 largest cities in the Northern Hemisphere to explore how urban-rural differences in species composition, topography, and climate affect spring phenological responsiveness to urbanization. To uncover the mechanisms driving the observed large-scale patterns, we conducted experiments in Beijing, focusing on phenological differences between urban and rural areas across four tree species commonly found in both settings. Of these species, three are predominantly urban, while one is more common in rural areas. Moreover, using high-resolution remote sensing data from Beijing, we compared how urbanization influences spring phenology at both the broader vegetation and individual species levels. We expected that species composition would influence the temperature sensitivity of spring phenology (S_T, expressed as change in days per degree of warming, d °C^{-1}) due to interspecific differences in S_T or distinct responses of species to urbanization. Therefore, urban-rural differences in species composition should contribute to variation in S_T between urban and rural vegetation.

Results and discussion
Effect of urban-rural variation in species composition on spring phenological responsiveness
We investigated the temperature sensitivity of tree phenology across urban and rural areas by studying phenological variation in 135 Northern Hemisphere cities[24]. Using the MODIS Global Vegetation Phenology product[25], we obtained start-of-season (SOS) dates from 2003 to 2020 at 500 m spatial resolution. For each city, we distinguished between urban and rural areas based on predefined city boundaries and proportionate outward extensions (see "Methods" and Supplementary Fig. 1a)[10,26]. In 97% of the cities, spring temperatures in urban areas were significantly higher than those in rural counterparts ($p < 0.1$), with an average difference of 0.30 ± 0.02 °C, ranging from 0.1 °C to 2.2 °C (Supplementary Fig. 2). Consistent results were

observed for mean annual temperatures (Supplementary Fig. 3). In 66% of cities, the SOS occurred earlier in urban areas than in rural areas, with an average difference of 6.5 ± 0.9 days (Fig. 1a and Supplementary Fig. 4). This finding is consistent with a previous study, which reported a difference of 6.1 ± 0.7 days[10].

We calculated the S_T of each pixel by analyzing the linear relationship between each year's SOS and preseason temperature from 2003 to 2020[15,27], which reflects the change in the SOS date per degree of warming (days °C^{-1}). For 60% of the analyzed pixels, preseason temperature significantly ($p < 0.1$) affected SOS (Supplementary Fig. 5). Subsequent analyses focused on these significant pixels, though results remained consistent when all pixels were included (Supplementary Figs. 5, 6). S_T was higher in urban than in rural areas for 51% of cities, with an average difference of 0.69 ± 0.24 d °C^{-1} (Fig. 1b and Supplementary Fig. 5a, b). Using all pixels, S_T was higher in urban than in rural areas for 66% of cities, with an average difference of 0.35 ± 0.11 d °C^{-1} (Supplementary Figs. 5c, d, 6b). The urban-rural difference in S_T was especially pronounced in Asian cities (0.74 ± 0.24 d °C^{-1}) but was minimal in European (0.11 ± 0.27 d °C^{-1}) and American (0.14 ± 0.09 d °C^{-1}) cities (Fig. 1b, Supplementary Figs. 6b, 7), aligning with prior regional studies[10,16].

To understand how species composition might influence observed trends, we extracted 3.5 million urban tree observations from the Global Biodiversity Information Facility (GBIF)[28], the most comprehensive global urban biodiversity data network currently available. We used the beta diversity index to quantify species composition differences between urban and rural areas of each city[29,30]. These differences were most pronounced in Asian cities, then American cities, with European cities showing the least variation (Figs. 1c and Supplementary Fig. 8). A higher beta diversity strongly increased urban-rural differences in SOS (ΔSOS, Figs. 1d and Supplementary Fig. 6d) and S_T (ΔS_T, Fig. 1e and Supplementary Figs. 6e, 9a, b). The pronounced ΔS_T observed in Asia may thus result from substantial differences in species composition between urban and rural areas. This is consistent with prior studies highlighting extensive landscaping efforts in Chinese cities that introduce exotic tree species and enhance urban-rural differences in species composition[17,18]. As a result, cities with high beta diversity tend to exhibit more pronounced variation in phenological responses between urban and rural areas. Given that greater species diversity is associated with enhanced ecosystem resilience to climate warming[21], cities with higher beta diversity, such as those in Asia, may have an advantage in adapting to future climate changes. However, further studies are needed to comprehensively understand how urban beta diversity impacts the resilience of cities to climate change.

To understand the key drivers of phenological variation between urban and rural areas, we quantified the effects of beta diversity, species richness, climate, vegetation characteristics, and population density on ΔSOS and ΔS_T. Both the differences (Δ) between urban and rural areas and city-level averages were considered. After evaluating multicollinearity among variables using variance inflation factors[31,32], we selected nine key variables for our analysis. Using random forest models[32], urban-rural differences in preseason temperature (ΔTemperature) was identified as the top driver of ΔSOS (Supplementary Fig. 10a). Beta diversity emerged as the top driver of ΔS_T, followed by ΔTemperature (Fig. 2a). Urban-rural species richness differences (ΔRichness) had a small effect on ΔSOS and ΔS_T, suggesting that phenological differences between urban and rural areas are driven primarily by variations in species composition rather than species richness itself. Further examination through recursive partitioning analyses[32,33] confirmed beta diversity as the top driver of ΔS_T, with ΔTemperature and mean annual temperature influencing ΔS_T under certain conditions (Fig. 2b). Specifically, in cities with high dissimilarity in species composition between urban and rural areas (beta diversity ⩾ 0.73), a warmer mean annual temperature is associated with a larger ΔS_T.
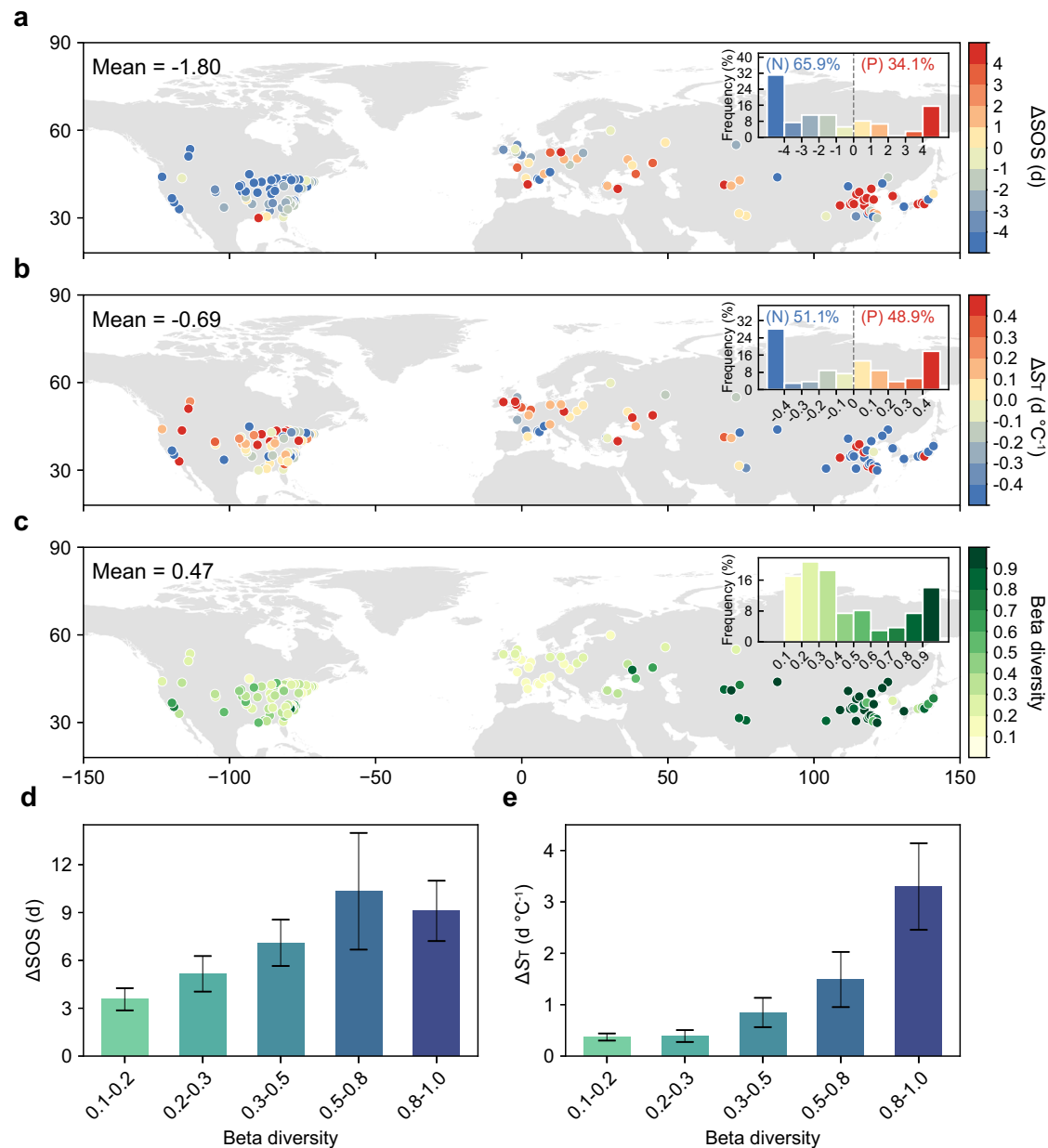
Fig. 1 | Effects of urban-rural differences in species composition (beta diversity) on urban-rural variation in the start-of-growing season (ΔSOS) and the temperature sensitivity of SOS (ΔS$_T$) using the outward delineation method. **a**, **b** Maps showing the urban-rural differences in SOS (ΔSOS) and S$_T$ (ΔS$_T$) for the selected 135 cities. **c** Maps showing the urban-rural variation in beta diversity. **d**, **e** Effects of beta diversity on absolute ΔSOS (mean ± se, **d**) and ΔS$_T$ (mean ± se, **e**).

The beta diversity index was grouped into five subsets based on the number of cities in each group (Supplementary Fig. 9a). There are 26, 26, 37, 18 and 28 cities in each beta diversity group from 0.1 to 1.0, respectively. Data underlying the figures are available on Zenodo (https://zenodo.org/records/14864842) and in the Source Data file.

Conversely, in cities with lower beta diversity (<0.73), a larger ΔTemperature leads to an increased ΔS$_T$.

To test whether the definition of urban and rural areas affected our findings and mitigate a potential bias due to fewer tree observation records in rural areas, we conducted an additional analysis comparing the inner, highly urbanized areas of cities to their outer, more rural parts within the city limits (inward delineation, Supplementary Fig. 1b). This approach revealed consistent patterns and corroborated the initial analysis, which treated all areas within city boundaries as urban (Supplementary Figs. 9c, d, 10–13). These findings show that differences in species composition between urban and rural areas largely drive variation in spring phenological responsiveness.

Species-specific responsiveness of spring phenology to urbanization

To investigate the mechanisms by which beta diversity influences the responsiveness of spring phenology to urbanization, we conducted species-level experiments in Beijing, China. With a population of ~21.9 million, Beijing has undergone extensive urban expansion and warming in recent decades[8,34]. To represent different levels of urbanization, Beijing was divided into six concentric zones (Zones 1 to 6) based on its ring roads (Supplementary Fig. 14). The city center (zone 1) of Beijing is 0.4 °C (March to May temperature, Spring T) warmer than its most rural area (zone 6, Fig. 3a). To analyze spring phenology along this urbanization gradient, we used the Landsat-based enhanced
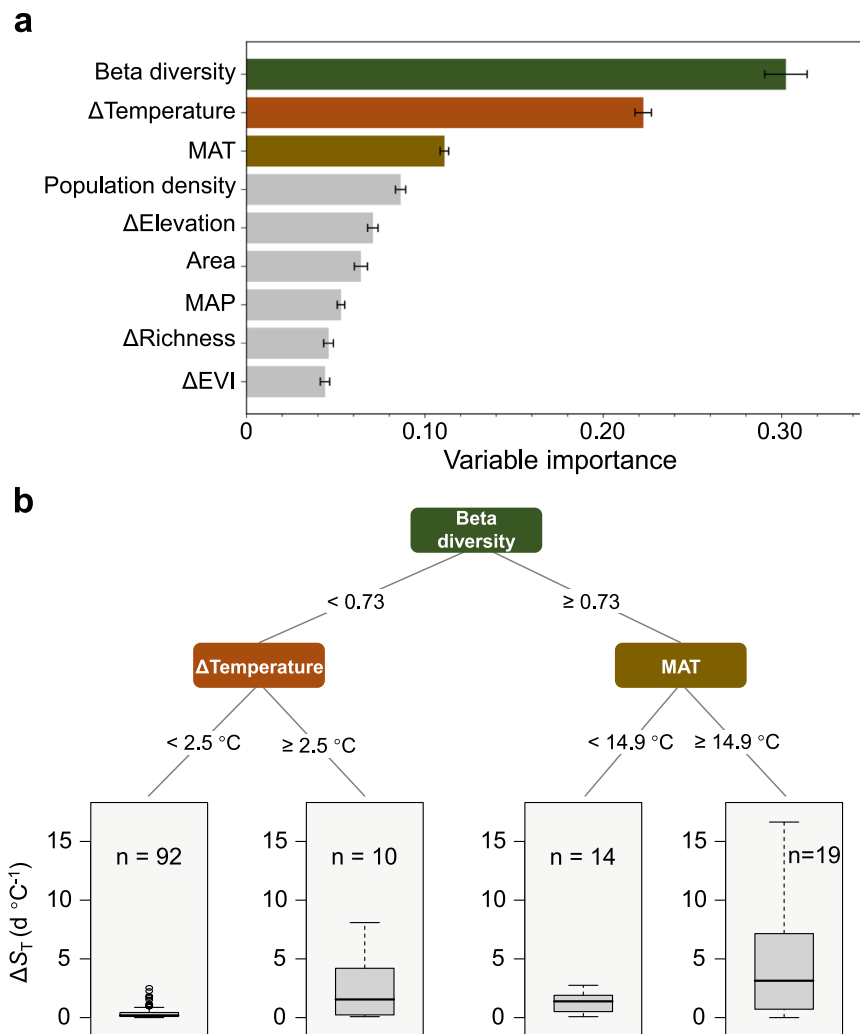
a

b

Fig. 2 | Drivers of urban-rural variation in temperature sensitivity of the start of season (ΔS_T). a Variable importance metrics (mean ± se) from random forest models for the effects of urban-rural differences in species composition (beta diversity), species richness (ΔRichness), preseason temperature (ΔTemperature), enhanced vegetation index (ΔEVI), geography (ΔElevation), the city-level averages of mean annual temperature (MAT) and precipitation (MAP), population density and city area on absolute ΔS_T using the outward delineation method ($n = 135$). **b** Recursive partitioning tree for the effects of beta diversity, absolute ΔTemperature and MAT on absolute ΔS_T. The boxes span from the first to the third quartile, with medians marked by black lines in the middle. The whiskers extend from the 5th to the 95th percentile. Data underlying the figures are available on Zenodo (https://zenodo.org/records/14864842) and in the Source Data file.

vegetation index (EVI) from 2003–2020. The SOS was defined as the date when EVI first crossed 50% of its annual peak (SOS$_{50}$). To exclude potential elevational effects due to mountains in the west of Beijing, we removed pixels with elevations higher than the mean ± 1.5 standard deviations of all pixels (268 m a.s.l.). In urban areas, the average SOS occurred on May 3, 15 days ahead of the SOS in rural areas on May 18 (Fig. 3b). Consistent with the Northern Hemisphere-wide trends (Fig. 1b), urban areas in Beijing displayed greater S_T, increasing from 2.1 to 4.4 d °C^{-1} compared to rural areas (Fig. 3c).

We assessed the urbanization impact on spring leaf-out at the species level by collecting twigs from three species dominant in urban areas (*Ginkgo biloba*, *Acer truncatum* and *Platanus occidentalis*) and one species common in rural areas (*Fraxinus chinensis*). Samples were collected from both rural (Jiufeng Mountain, outside zone 6) and urban (Beijing Zoo, in zone 2) locations (see "Methods" and Supplementary Fig. 14). These twigs, collected at two different dormancy stages, were exposed to the full combination of four temperature (5, 10, 15 and 20 °C) and two photoperiod treatments (8 and 16 h) in controlled climate chambers[35]. Contrary to the vegetation-level observations, no difference in S_T was found between urban and rural plants when grouping all species (Fig. 3e), implying that the

vegetation-level results are driven by urban-rural variation in species composition. Furthermore, the experiments showed that the effect of urbanization on S_T differed significantly among species (Fig. 3e). Except for *Platanus*, which showed similar S_T in urban and rural areas (Urban $S_T = -6.2 \pm 0.4$ °C^{-1}; Rural $S_T = -6.4 \pm 0.4$ d °C^{-1}), urban-dominant species (*Ginkgo* and *Acer*) exhibited higher S_T in urban than in rural areas (*Ginkgo*: Urban $S_T = -5.7 \pm 0.4$; Rural $S_T = -5.1 \pm 0.3$ d °C^{-1}; *Acer*: Urban $S_T = -6.5 \pm 0.2$; Rural $S_T = -5.7$ d ± 0.1 °C^{-1}). In contrast, the rural-dominant species exhibited the opposite response (*Fraxinus*: Urban $S_T = -5.5 \pm 0.4$; Rural $S_T = -7.6 \pm 0.4$ d °C^{-1}). ANOVA results confirmed a significant effect of species on S_T, and, importantly, also showed a strong interaction between species and urbanization, suggesting that the effect of urbanization on S_T depends on the species (Supplementary Table. S1). This supports the fundamental role of species composition in driving variation in S_T between urban and rural areas.

Using high-resolution Landsat imagery, we validated our experimental findings by analyzing satellite-derived spring phenology for each of the four tree species in both urban (zone 1 and 2) and rural areas (zones 5 and 6). The satellite-derived results were consistent with the experiment, with *Ginkgo* and *Acer* showing significantly higher S_T in
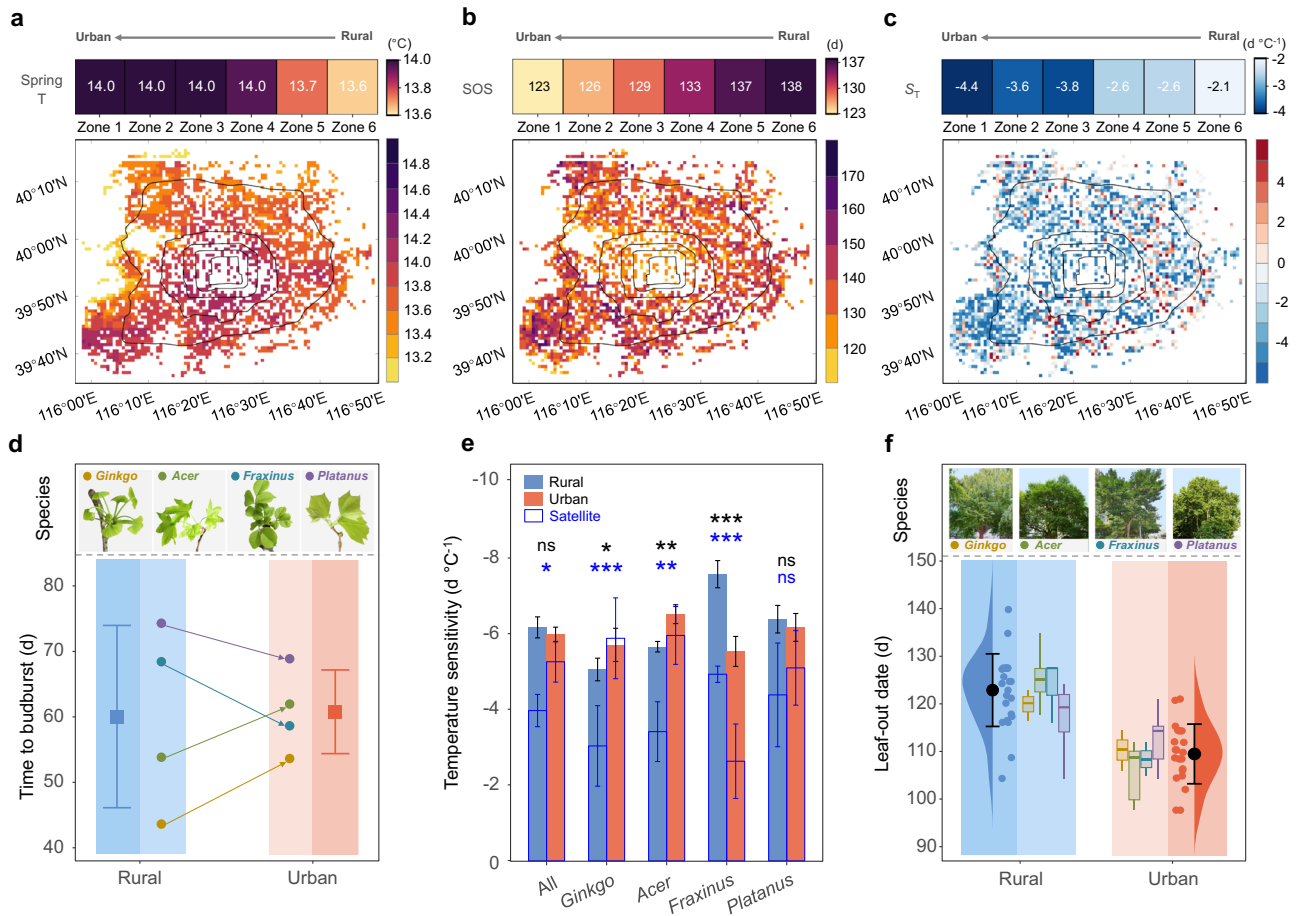
Fig. 3 | Experimental evidence for the effects of urbanization on spring phenology. a–**c** Effects of urbanization on spring temperature (Spring T, **a**), the start-of-season (SOS, **b**) and the temperature sensitivity of SOS (S_T, **c**). Pixels with elevations higher than the mean ± 1.5 standard deviations of all pixels (268 m a.s.l.) were excluded. The black lines indicate the rings 2–6 in Beijing, which divide the study area into six concentric zones (Zone 1 to Zone 6). **d** Effects of urbanization on spring phenology based on a manipulative experiment at the species level using twig cuttings and climate chambers. The dots indicate the average time to budburst of each species when growing in a rural or urban area ($n = 16$), respectively. The squares and error bars indicate the average budburst dates and its standard deviation across species ($n = 64$). **e** Effects of urbanization on the sensitivity of spring phenology to temperature using either twig cutting experiments or individual-based satellite images at the species level. The temperature sensitivities were estimated from the manipulative experiments (solid bars, $n = 32$) or the

satellite-based observations (bars with blue lines, $n = 45$). The error bars indicate the standard error of the mean. The asterisks and "ns" indicate the significance levels determined by a two-sided t-test: ns, not significant; *, $p < 0.1$; **, $p < 0.05$ and ***, $p < 0.01$. **f**, Effects of urbanization on spring phenology using individual-based satellite observations at the species level. To obtain species-level observations, patches where one of the four tree species was dominant were selected ($n = 45$). Dots refer to the spring phenology of each patch, the semi-violin plots indicate the distribution of spring phenology, and the error bar refers to the standard deviation of spring phenology. Species-specific results are presented as boxplots, with medians marked by black lines in the middle and the 25th and 75th percentiles as bounds. Whiskers extend from the 5th to the 95th percentiles. *Ginkgo*, *Acer*, *Fraxinus* and *Platanus* refer to *Ginkgo biloba*, *Acer truncatum*, *Fraxinus chinensis* and *Platanus occidentalis*, respectively. Data underlying the figures are available on Zenodo (https://zenodo.org/records/14864842) and in the Source Data file.

urban than in rural areas, while *Fraxinus* showed the opposite trend (Fig. 3e). Additionally, our twig-cutting experiment revealed varied effects of photoperiod and chilling on species' spring phenology and their degree-day requirements (Supplementary Figs. 15, 16). Specifically, *Fraxinus* was influenced by day length and unaffected by chilling, whereas *Ginkgo* and *Acer* were more strongly affected by chilling, possibly accounting for the observed variation in S_T among the species[36,37]. These results highlight the substantial influence of species-specific phenological differences on the satellite-derived results at the vegetation level.

Based on our species-level observational and experimental data, we propose two mechanisms for how species-specific phenological responsiveness to urbanization may affect the urban-rural variation in vegetation-level S_T. First, inherent temperature sensitivities vary among species, meaning that differences in species composition between urban and rural areas directly contribute to differences in

temperature sensitivity (Fig. 4a). Second, the effect of urbanization on S_T depends on the species. For instance, should urbanization-driven warming reduce S_T of species A but increase it in species B (Fig. 4b), vegetation-level S_T remains constant across urban and rural areas when both species are equally abundant in urban and rural areas (Fig. 4c, *Scenario* 1, $S_{T\_urban} = S_{T\_rural}$). Conversely, S_T will decline in urban areas if species A is predominantly found there (*Scenario* 2, $S_{T\_urban} < S_{T\_rural}$), whereas S_T will increase in urban areas if species B is more dominant (*Scenario* 3, $S_{T\_urban} > S_{T\_rural}$).

These findings demonstrate that variation in species-specific temperature sensitivities, combined with species-specific responses to urbanization, drive the observed urban-rural differences in vegetation-level phenological temperature sensitivity. While we aimed to include species representative of the dominant trees in urban and rural settings, we acknowledge that other species may exhibit different patterns, warranting further investigation.
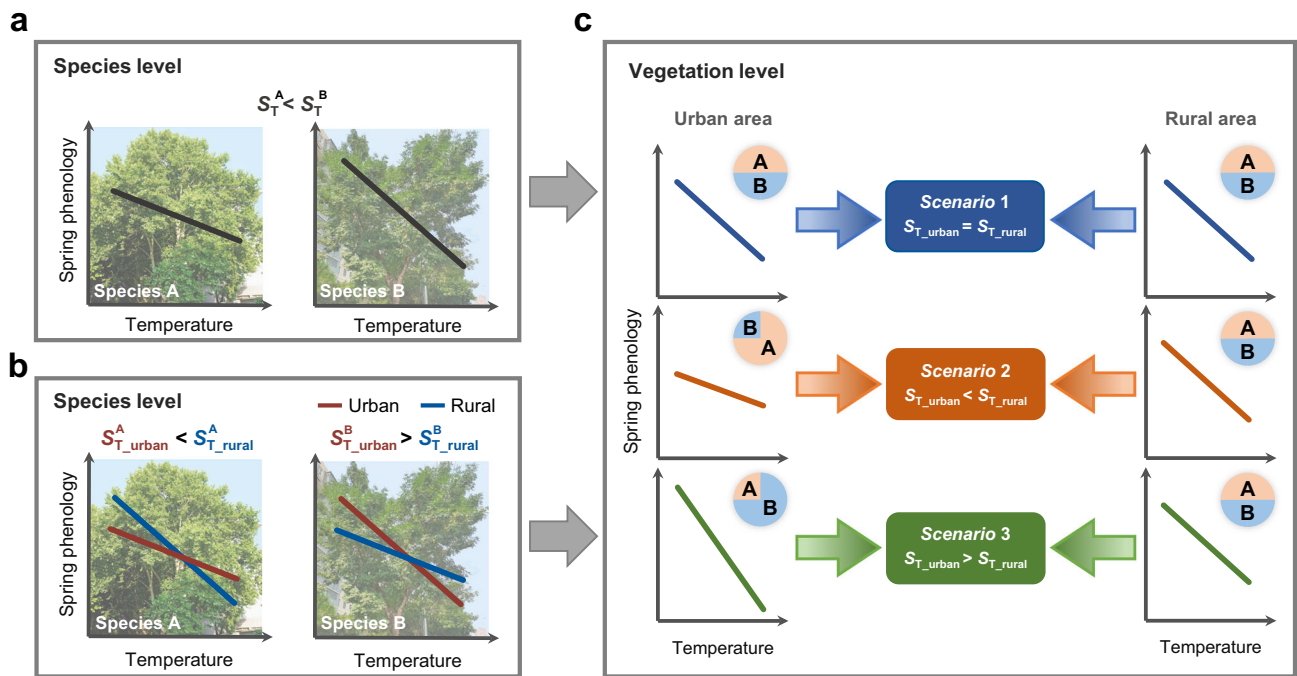
Fig. 4 | Conceptual diagram of how differences in the phenological responsiveness among species may affect the urban-rural variation in temperature sensitivity of spring phenology (S_T) at the vegetation level. Variation in S_T across species (**a**) and/or variation in the effect of urbanization on S_T across species (**b**) will cause variation in vegetation-level S_T between urban and rural areas if species composition differs (scenarios 2 and 3 in panel **c**). If S_T of species A is lower than that of species B (**a**), no significant difference in vegetation-level S_T will be observed between urban and rural areas if species A and B are equally abundant in urban and rural areas (*Scenario* 1 in **c**). However, if species A becomes more abundant in urban areas, then S_T will decline in urban areas (*Scenario* 2). By contrast, if species B is dominant in urban areas, then S_T will increase in urban areas (*Scenario* 3). The same variations in vegetation-level S_T between urban and rural areas in response to species composition shifts (**c**) will be observed in a scenario where urbanization-induced warming reduces S_T of species A but increases it in species B (**b**). Data underlying the figures are available on Zenodo (https://zenodo.org/records/14864842) and in the Source Data file.

Implication of the findings

Our study underscores the critical role of species composition in shaping urban-rural variations in the temperature sensitivity of spring phenology, with significant implications for urban ecology and climate change research.

1. Refining phenological predictions: The strong influence of species composition suggests that satellite-derived phenology along urbanization gradients may not accurately reflect individual species' responses to climate change. Integrating species-specific data into phenological studies is essential for improving predictions of ecosystem responses to warming.

2. Cascading ecological effects: Our findings suggest that community structure strongly influences plant phenology[21,38], potentially leading to interspecific mismatches that can disrupt trophic interactions, such as those between plants and pollinators or predators and prey[39,40]. These mismatches can cascade through ecosystems, affecting population dynamics and functions like carbon sequestration and nutrient cycling[40,41]. Incorporating these dynamics into vegetation models is critical for improving predictions of future carbon and water cycles.

3. Urban ecology as a research framework: Urban areas are frequently used as proxies for studying climate change impacts due to their elevated temperatures and CO_2 concentrations. However, ignoring species composition may lead to inaccurate predictions of ecosystem responses[12]. By recognizing the importance of community structure, urban ecologists can better leverage cities as "natural laboratories" to explore ecosystem functioning and the ecological consequences of urbanization.

4. Practical insights for urban planning: Strategic management of urban species composition offers actionable solutions for mitigating urban heat island effects, stabilizing microclimates, and reducing

temperature extremes. These nature-based approaches enhance urban resilience to climate change and align with broader sustainability goals, providing cities with pathways to address ecological challenges while adapting to warming climates.

Our study reveals the large influence of species composition on urban-rural variations in spring phenological responsiveness to temperature. We show that greater differences in species composition between rural and urban regions correlate with greater urban-rural differences in temperature sensitivity of spring phenology, as supported by both experimental and satellite-derived data. The contrasting temperature sensitivities among species and their varied responses to urbanization are primary drivers of these patterns, emphasizing the need to account for species composition in urban phenological studies[1,6,26]. Relying solely on satellite data without considering these differences may result in skewed interpretations, particularly in regions like Asia, where significant contrasts in species composition are driven by climate, soil conditions, and human activity[42,43]. While our analysis leveraged the comprehensive GBIF dataset to capture species composition differences, we acknowledge its limitations, such as sparse observations in some urban areas. Expanding datasets on species diversity will be crucial for advancing this field. Additionally, although our study focused on trees due to their ecological importance and the relative ease of assessing their diversity, future research should consider other vegetation types to gain a more comprehensive understanding of urban phenology. Our findings highlight the importance of species-specific responses to climate change in shaping vegetation-level trends, with potential implications for phenological mismatches that could disrupt ecosystems as the climate warms[44]. Ultimately, climate-driven changes in species composition and species-specific phenological responses will need to be considered for accurate predictions of ecosystem functioning under climate change.

Methods

Analysis of satellite-derived phenology observations at city level

Urban boundary data. The urban area boundaries were determined using the latest version of the Global Urban Boundaries (GUB) dataset (http://data.ess.tsinghua.edu.cn)[24]. The dataset was obtained from 30 m resolution Landsat imagery, employing a hierarchical approach to improve the homogeneity of built-up areas within urban centers while preserving the heterogeneity of built-up areas at the urban fringes[24]. We extracted data for the 300 large cities across the Northern Hemisphere, spanning from 30° to 90°N latitude. After quality checks and data matching with phenology datasets, a total of 285 cities, with an area between 157 to 5117 km², were included in further analysis.

Tree species observation data. Our georeferenced species' occurrences were obtained from the Global Biodiversity Information Facility (GBIF; https://www.gbif.org), an international network and data infrastructure that provides open access to data encompassing all forms of life on Earth[28]. The GBIF dataset stands as the world's largest biodiversity data network[45] and has been extensively used in biodiversity and phenology studies[46], allowing us to conduct this study at a global scale. We obtained tree species occurrences following these steps: i) we removed the records from living specimens and conserved specimens; ii) queried all tracheophyte species and extracted georeferenced data records, excluding any coordinates with an abnormal latitude and longitude range; iii) standardized and harmonized scientific names of tracheophytes using the R package U.Taxonstand[47]; iv) extracted all tree species occurrence records for the urban and rural areas of the selected cities.

Phenology data. Start-of-season (SOS) dates for the period 2003–2020 were obtained from the MODIS Global Vegetation Phenology product (MCD12Q2 V6)[25]. This product provides phenological metrics at a spatial resolution of 500 m for every vegetated pixel on land, derived from time series of the 2-band Enhanced Vegetation Index (EVI2). SOS was defined as the date when EVI2 first crossed 50% of the segment EVI2 amplitude greenness. We extracted multi-year SOS data for all pixels within the urban-rural extent. To reduce uncertainties, we removed pixels i) in which SOS occurred before March 1 or after May 31, and ii) with phenology information available for fewer than 15 years.

Climate geography data. We obtained daily near-surface air temperature data at 1-km resolution from ref. 48. Additionally, 30-year mean annual temperature and precipitation data were obtained from CHELSA V2.1 (Climatologies at High resolution for the Earth Land Surface Areas, https://chelsa-climate.org/)[49], hosted by the Swiss Federal Institute for Forest, Snow, and Landscape Research WSL. Elevation data was derived from EarthEnv (https://www.earthenv.org/topography), which is based on the digital elevation model products of global 250 m GMTED2010 and near-global 90 m SRTM4.1dev[50]. Human density data were derived from the Gridded Population of the World product[51], using 2020 as the reference year.

Vegetation data. The vegetation classification dataset was derived from the MODIS Land Cover Type (MCD12Q1) Version 6.1 data product (https://lpdaac.usgs.gov/products/mcd12q2v061/). This product provides global land cover types at yearly intervals, with 2011 used as the reference year in this study. Vegetation types, including cultivated croplands and grasslands, were excluded from the analyses[10]. Enhanced Vegetation Index (EVI) data were derived from Aqua Moderate Resolution Imaging Spectroradiometer (MODIS) Vegetation Indices (MYD13Q1) Version 6.

Statistical analysis. To compare vegetation responses between urban and rural areas, we defined urban areas as the regions within the established city boundaries for each city. Rural areas were defined as a proportionate outward extension of these boundaries, meaning the rural area boundary is symmetrically and evenly expanded in size and shape to cover the same area as the predefined urban portion of the city (outward delineation, Supplementary Fig. 1a)[10,26]. Alternatively, we used inward delineation, where urban and rural areas were represented by inner and outer polygons of equivalent area within the city boundary (inward delineation, Supplementary Fig. 1b). This dual delineation allowed us to test the robustness of our findings and account for potential biases arising from variations in tree observation records and sampling efforts across urban and rural zones. These paired urban and rural areas were used in subsequent analyses. To avoid potential bias from small sample sizes of tree observations in some cities, we excluded cities with fewer than 500 tree records in either rural or urban areas. Consequently, 135 cities (>1000 tree records) were retained for the outward strategy, and 115 cities for the inward strategy, both of which were used in the final analysis.

To compare the difference in species composition between urban and rural areas, we calculated beta diversity as the Bray-Curtis difference using the number of individuals per species[30]. The R package vegan 2.6-4 provides functions for calculating beta diversity[52].

We defined the preseason as the 90 days preceding the mean SOS date for each pixel[53], and calculated the mean temperature during the preseason for each year. We calculated the S_T of each pixel by analyzing the linear relationship between each year's SOS and preseason temperature from 2003 to 2020[15,27], which reflects the change in the SOS date per degree of warming (days °C^{-1}). We further calculated the mean SOS and S_T for both rural and urban areas (SOS$_{rural}$, SOS$_{urban}$, S_{T_rural} and S_{T_urban}). The difference in SOS (ΔSOS) and S_T (ΔS_T) was calculated to present the variation in SOS and S_T between urban and rural areas. Based on the sample size (number of cities), we grouped the beta diversity index into 5 or 6 subsets at different beta diversity intervals to examine the effects of beta diversity on ΔSOS and ΔS_T (Supplementary Fig. 9). Variance inflation factor (VIF) analysis was used to examine the multicollinearity among variables[32], including beta diversity, and both the urban-rural differences (Δ) and the city-level averages of climate factors (preseason temperature, mean annual temperature, and mean annual precipitation), topography (elevation and area), vegetation (species richness and EVI), and human-related factors (population density) between urban and rural areas. After excluding highly correlated variables, all VIFs were smaller than 5, suggest sufficient independence among the predictors. We selected nine key variables for our analysis and assessed their relative importance using random forest models[32]. To further explore the interactive effects among the main drivers of ΔS_T, we conducted recursive partitioning analyses using the 'partykit' and 'ggparty' packages[32,33]. Using a decision tree algorithm, we investigated the context dependency for the effects of the variables on absolute ΔS_T. The minimum node size was set to ~20% (27 data points for the outward strategy and 23 for the inward strategy) of the total city number.

Climate-controlled experiment and high-resolution satellite-based observations at species level

Study area. Beijing is one of the largest cities around the world with a population of 21.9 million (115.7-117.4 °E, 39.4-41.6 °N, Supplementary Fig. 14), and has experienced extensive expansion and intensive warming in recent decades[8,34]. Beijing is characterized by a warm, temperate monsoon climate, with an average annual temperature of 11–13 °C and an average annual precipitation of ~600 mm. Precipitation is high in summer, while winters are cold and dry. The dominant vegetation type is broad-leaved deciduous forest. Based on the ring roads of Beijing, we divided the study area into six concentric zones (Zones 1 to 6, Supplementary Fig. 14) to roughly reflect the degrees of urbanization following previous studies[34,54].

Vegetation phenology using remote sensing. The SOS was estimated using long-term Landsat images from 2003 to 2020 via the Google Earth Engine (GEE) platform following Li et al. (2017, 2019). We used atmospherically corrected surface reflectance Landsat images (Level 2, Collection 2) from different sensors (Thematic Mapper, Enhanced Thematic Mapper Plus and Operational Land Imager) at 30 m spatial and 16-day temporal resolution. Previous studies indicated that the enhanced vegetation index (EVI) improves the estimation of spring phenology relative to the Normalized Difference Vegetation Index (NDVI) in temperate regions[55], and we thus used the EVI to quantify spring phenology. We then created a composite of the EVI time series for each pixel[56,57], and applied a masking procedure to remove clouds and shadows[58].

To capture the seasonal patterns of vegetation dynamics, we selected clear-sky observations of EVI at each pixel (30 m × 30 m) and ordered them by the day of year (DOY). To minimize the impact of abnormal observations, we applied a moving average method to the continuous observations. A double logistic model was then applied to fit the time series of EVI curves to characterize the seasonal change of vegetation growth as follows:

$$f(t) = v_1 + v_2 \left(\frac{1}{1+e^{-m_1(t-n_1)}} - \frac{1}{1+e^{-m_2(t-n_2)}} \right)$$

where $f(t)$ represents the fitted EVI value at DOY t; v_1 and v_2 refer to the background and amplitude of EVI over the year; n_1 and n_2 refer to the dates of maximum increase or decrease in EVI based on sigmoid curves, and m_1 and m_2 are the slopes that determine the shape of the sigmoid curves. The parameters were estimated using a stepwise statistical approach[57].

Consistent with MODIS phenology dataset, the SOS was defined as the date when the EVI first reaches 50% of its annual amplitude (SOS_{50}). We extracted vegetation SOS for Beijing from MODIS and Landsat data, and matched their resolutions to 500 m (Supplementary Figs. 17a, b). The SOS derived from Landsat was highly correlated with that from MODIS, indicating consistency between the two datasets ($r = 0.73$, Supplementary Fig. 17c). To exclude potential elevational effects due to mountains in the west of Beijing, we removed pixels with elevations higher than the mean ± 1.5 standard deviations of all pixels (268 m a.s.l.). We used the MODIS Land Cover Type data product to exclude cultivated croplands and grasslands. Daily near-surface air temperatures were extracted from a global gridded dataset with a spatial resolution of 1 km covering the period from 2003 to 2020 (https://doi.org/10.25380/iastate.c.6005185)[48]. The elevation data for Beijing was derived from the 30 m resolution NASADEM dataset (https://earthdata.nasa.gov/esds/competitive-programs/measures/nasadem), which was used to exclude mountain pixels.

Species-level phenology using a manipulative experiment. Twigs of four tree species were collected from a rural (Jiufeng Mountain, outside zone 6, 30 km away from the city center) and an urban area (Beijing Zoo in the city center in zone 2, Supplementary Fig. 14). The temperature sensors installed at the two collection sites showed that the daily air temperature in the urban area was 4.5 °C higher than in the rural area, with an average annual temperature of 13.6 and 9.1 °C, respectively (Supplementary Fig. 18).

Based on the List of Major Native Tree Species in Beijing and GBIF observations, we selected four common temperate deciduous tree species: three of them dominant in urban areas (*Ginkgo biloba*, *Acer truncatum*, and *Platanus occidentalis*) and one predominant in rural areas (*Fraxinus chinensis*) (hereafter referred to as *Ginkgo*, *Acer*, *Fraxinus* and *Platanus*). We selected twelve healthy adult individuals for each of the four species, with six individuals sampled from Jiufeng Mountain and six from Beijing Zoo, yielding a total of 48 tree individuals (6 individuals × 4 species × 2 sites). All the selected trees were

mature and had similar diameters at breast height. Eight healthy twigs ~40 cm in length were cut from each individual tree (from the southern side of the canopy) in December 2020 and January 2021, respectively. We disinfected the twigs with commercial hypochlorite solution and then placed them in 395 ml plastic bottles filled with 265 ml cool tap water. After pre-processing, we transferred the twigs to climate chambers, recut them by ~2 cm at the base every two weeks to avoid the occlusion of vessels, and changed the water in the bottles every one to two weeks[37].

The experiment consisted of 16 combinations of environmental treatments (2 chilling × 4 temperature × 2 photoperiod) using 768 twigs. Four constant temperature treatments, i.e., 5 °C (T5), 10 °C (T10), 15 °C (T15) and 20 °C (T20) were implemented in four climate chambers. In each chamber, two photoperiod treatments (8 and 16 h) were applied to test whether photoperiod had any effect on budburst time by covering half the space of the chambers with shade cloth every day[35]. Furthermore, two chilling treatments were applied by collecting twigs earlier and later in winter, causing different exposure of twigs to outdoor winter conditions[37,59] (December 31, 2020 [Low chilling, C_{low}] and January 19, 2021 [High chilling, C_{high}]). The environmental treatment of this experiment lasted from January 1, 2020, to June 3, 2021. Temperature sensors (HOBO MX2202, Onset Computer Corporation, Bourne, MA, USA) were used to record the air temperature of each environmental treatment every 30 minutes (Supplementary Fig. 19). Illuminance in all chambers was ~8944 lux (161 μmol m^{-2} s^{-1}), the average concentration of CO_2 was ~442 ppm, the relative air humidity was ~40%.

For each cultivated twig, we monitored the development of buds every three days and recorded the budburst date, which was defined as the date when the bud scale opened and the leaf was partially visible[37,60]. Spring phenology was then represented using the days to achieve budburst, defined as the number of days from the date of treatment start to the budburst date. The heat requirement (growing degree days, GDD) for each twig to achieve budburst was calculated using the mean daily temperature, with a base temperature set at 0 °C.

Species-level phenology using remote sensing. To validate the results of the twig-cutting experiment, we used 30 m resolution Landsat images to extract the SOS for the same species and conducted further species-level analysis. We selected 3-10 patches (dominated by one of the four species used in the twig-cutting experiment) at rural areas (zones 5 and 6; Fenghuang Mountain, 116°05′30″E, 40°06′46″N; Jiufeng Mountain, 116°5′11″E, 40°03′42″N; Xishan Forest Park, 116°12′36″E, 39°58′40″N) and urban areas (zone 2; Beijing Normal University, 116°22′20″E, 39°58′02″N; Beijing Zoo, 116°20′36″E, 39°56′52″N; Yuyuantan Park, 116°19′35″E, 39°55′21″N). Latitude and longitude of the patches were recorded using a hand-held GPS to extract Landsat and climate data for the respective sites. We then extracted the spring phenology dates of each patch for each species using the same methodology used for the vegetation-level phenology analysis.

Statistical analysis. We first analyzed the effects of urbanization on spring temperature (from March to May, Spring T), spring vegetation phenology (SOS) and the sensitivity of spring phenology to temperature (S_T) along the urbanization gradients. To compare the vegetation-level phenology results with species-level patterns, we additionally analyzed the effects of urbanization on spring phenology using the observations from the manipulative experiment and species-level vegetation phenology. The temperature sensitivity of spring phenology (S_T, defined as the advancement in budburst date per degree warming, days °C^{-1}) was calculated using linear regression analysis[35]. For the manipulative experiment, the air temperature of each chamber was used to calculate the S_T. For the satellite-derived SOS, we defined the preseason as the 90 days preceding the mean SOS date for each

pixel[53], and calculated the mean temperature during the preseason for the S_T calculation. The difference in spring phenology and growing degree days between rural and urban areas was tested using the paired t-test, ANCOVA was used to test for S_T differences among treatments. ANOVA was conducted to test the effects of species and urbanization on S_T, with species, urbanization, chilling and photoperiod treatments as explanatory variables and S_T as response variable. Two models were employed: Model 2 included these variables as predictors, while Model 1 extended to involve the interaction of species and site as predictors (Supplementary Table. 1).

Reporting summary
Further information on research design is available in the Nature Portfolio Reporting Summary linked to this article.

Data availability
Urban area boundary data is publicly available from the Global Urban Boundaries (GUB) (http://data.ess.tsinghua.edu.cn). Species' occurrences data is publicly available from the Global Biodiversity Information Facility (GBIF; https://www.gbif.org). Vegetation phenology data is publicly available from the MODIS Global Vegetation Phenology product (MCD12Q2 V6, https://lpdaac.usgs.gov/products/mcd12q2v006/). The daily near-surface air temperature data is publicly available from Iowa State University (https://iastate.figshare.com/collections/A_global_1_km_resolution_daily_near-surface_air_temperature_dataset_2003_2020_/6005185). The vegetation classification dataset is publicly available from the MODIS Land Cover Type (MCD12Q1) Version 6.1 data product (https://lpdaac.usgs.gov/products/mcd12q2v061/). Mean annual temperature and precipitation data is publicly available from CHELSA V2.1 (https://chelsa-climate.org/). Topography data is publicly available from EarthEnv (https://www.earthenv.org/topography). Human density data is publicly available from the Gridded Population of the World product (https://sedac.ciesin.columbia.edu/data/collection/gpw-v3). Normalized Difference Vegetation Index (NDVI) and Enhanced Vegetation Index (EVI) data are publicly available from Aqua Moderate Resolution Imaging Spectroradiometer (MODIS) Vegetation Indices Version (MYD13Q1, https://lpdaac.usgs.gov/products/myd13q1v006/). Tree cover data is publicly available from the Global Land Analysis and Discovery product (https://glad.umd.edu/Potapov/TCC_2010/). Tree density data is publicly available from ref (https://www.nature.com/articles/nature14967). The elevation data for Beijing is publicly available from the 30 m resolution NASADEM dataset (https://earthdata.nasa.gov/esds/competitive-programs/measures/nasadem). Data underlying the figures are available on Zenodo[61] (https://zenodo.org/records/14864842). Source data are provided as a Source Data file. Source data are provided with this paper.

Code availability
All code used for data analysis is available at https://github.com/Phenodoge/Urban_phenology and Zenodo[62] (https://doi.org/10.5281/zenodo.15025737).

References
1. Körner, C. & Basler, D. Phenology under global warming. *Science* **327**, 1461–1462 (2010).
2. Vitasse, Y. et al. The great acceleration of plant phenological shifts. *Nat. Clim. Chang.* **12**, 300–302 (2022).
3. Menzel, A. et al. Climate change fingerprints in recent European plant phenology. *Glob. Change Biol.* **26**, 2599–2612 (2020).
4. Chuine, I. & Beaubien, E. G. Phenology is a major determinant of tree species range. *Ecol. Lett.* **4**, 500–510 (2001).
5. Peñuelas, J. & Filella, I. Responses to a warming world. *Science* **294**, 793–795 (2001).

6. Piao, S. et al. Plant phenology and global climate change: current progresses and challenges. *Glob. Change Biol.* **25**, 1922–1940 (2019).
7. Jia, W. et al. Urbanization imprint on land surface phenology: the urban–rural gradient analysis for Chinese cities. *Glob. Change Biol.* **27**, 2895–2904 (2021).
8. Zhou, Y., Li, X., Asrar, G. R., Smith, S. J. & Imhoff, M. A global record of annual urban dynamics (1992–2013) from nighttime lights. *Remote Sens. Environ.* **219**, 206–220 (2018).
9. Calfapietra, C., Peñuelas, J. & Niinemets, Ü. Urban plant physiology: adaptation-mitigation strategies under permanent stress. *Trends Plant Sci.* **20**, 72–75 (2015).
10. Meng, L. et al. Urban warming advances spring phenology but reduces the response of phenology to temperature in the conterminous United States. *Proc. Natl Acad. Sci. USA* **117**, 4228–4233 (2020).
11. Li, D., Stucky, B. J., Deck, J., Baiser, B. & Guralnick, R. P. The effect of urbanization on plant phenology depends on regional temperature. *Nat. Ecol. Evol.* **3**, 1661–1667 (2019).
12. Zhou, Y. Understanding urban plant phenology for sustainable cities and planet. *Nat. Clim. Chang.* **12**, 302–304 (2022).
13. Zohner, C. M. Phenology and the city. *Nat. Ecol. Evol.* **3**, 1618–1619 (2019).
14. Chamberlain, C. J. & Wolkovich, E. M. Variation across space, species and methods in models of spring phenology. *Clim. Change Ecol.* **5**, 100071 (2023).
15. Fu, Y. H. et al. Declining global warming effects on the phenology of spring leaf unfolding. *Nature* **526**, 104–107 (2015).
16. Wang, L. et al. Urban warming increases the temperature sensitivity of spring vegetation phenology at 292 cities across China. *Sci. Total Environ.* **834**, 155154 (2022).
17. Li, D., Wu, S., Liang, Z. & Li, S. The impacts of urbanization and climate change on urban vegetation dynamics in China. *Urban Forestry Urban Green.* **54**, 126764 (2020).
18. Yan, P. & Yang, J. Species diversity of urban forests in China. *Urban Forestry Urban Green.* **28**, 160–166 (2017).
19. Mori, A. S. et al. Biodiversity–productivity relationships are key to nature-based climate solutions. *Nat. Clim. Chang.* **11**, 543–550 (2021).
20. Chen, S. et al. Plant diversity enhances productivity and soil carbon storage. *Proc. Natl Acad. Sci.* **115**, 4027–4032 (2018).
21. Shen, P. et al. Biodiversity buffers the response of spring leaf unfolding to climate warming. *Nat. Clim. Chang.* **14**, 863–868 (2024).
22. Wohlfahrt, G., Tomelleri, E. & Hammerle, A. The urban imprint on plant phenology. *Nat. Ecol. Evol.* **3**, 1668–1674 (2019).
23. Zhou, D., Zhao, S., Zhang, L. & Liu, S. Remotely sensed assessment of urbanization effects on vegetation phenology in China's 32 major cities. *Remote Sens. Environ.* **176**, 272–281 (2016).
24. Li, X. et al. Mapping global urban boundaries from the global artificial impervious area (GAIA) data. *Environ. Res. Lett.* **15**, 094044 (2020).
25. Friedl, M., Gray, J. & Sulla-Menashe, D. MCD12Q2 MODIS/Terra +Aqua land cover dynamics yearly L3 global 500m SIN grid V006. https://doi.org/10.5067/MODIS/MCD12Q2.006 (2019).
26. Li, X. et al. Response of vegetation phenology to urbanization in the conterminous United States. *Glob. Change Biol.* **23**, 2818–2830 (2017).
27. Keenan, T. F., Richardson, A. D. & Hufkens, K. On quantifying the apparent temperature sensitivity of plant phenology. *N. Phytologist* **225**, 1033–1040 (2020).
28. GBIF.org. GBIF Occurrence Download. https://doi.org/10.15468/dl.s276bz (2023).
29. Zhang, C., He, F., Zhang, Z., Zhao, X. & von Gadow, K. Latitudinal gradients and ecological drivers of β-diversity vary across spatial

scales in a temperate forest region. *Glob. Ecol. Biogeogr.* **29**, 1257–1264 (2020).

30. Zhong, Y. et al. Arbuscular mycorrhizal trees influence the latitudinal beta-diversity gradient of tree communities in forests worldwide. *Nat. Commun.* **12**, 3137 (2021).

31. Wu, Z., Fan, C., Zhang, C., Zhao, X. & von Gadow, K. Effects of biotic and abiotic drivers on the growth rates of individual trees in temperate natural forests. *Ecol. Manag.* **503**, 119769 (2022).

32. Ma, H. et al. The global distribution and environmental drivers of aboveground versus belowground plant biomass. *Nat. Ecol. Evol.* **5**, 1110–1122 (2021).

33. Hothorn, T. & Zeileis, A. Partykit: a modular toolkit for recursive partytioning in R. *J. Mach. Learn. Res.* **16**, 3905–3909 (2015).

34. Wu, W., Zhao, S., Zhu, C. & Jiang, J. A comparative study of urban expansion in Beijing, Tianjin and Shijiazhuang over the past three decades. *Landsc. Urban Plan.* **134**, 93–106 (2015).

35. Wu, Z. et al. The sensitivity of ginkgo leaf unfolding to the temperature and photoperiod decreases with increasing elevation. *Agric. Meteorol.* **315**, 108840 (2022).

36. Fu, Y. H. et al. Daylength helps temperate deciduous trees to leafout at the optimal time. *Glob. Change Biol.* **25**, 2410–2418 (2019).

37. Wu, Z. et al. Poleward shifts in the maximum of spring phenological responsiveness of Ginkgo biloba to temperature in China. *N. Phytologist* **240**, 1421–1432 (2023).

38. Wu, X. et al. Canopy structure regulates autumn phenology by mediating the microclimate in temperate forests. *Nat. Clim. Chang.* 1–7 https://doi.org/10.1038/s41558-024-02164-2 (2024).

39. Benoit, A. D. & Kalisz, S. Predator effects on plant-pollinator interactions, plant reproduction, mating systems, and evolution. *Annu. Rev. Ecol., Evolution, Syst.* **51**, 319–340 (2020).

40. Renner, S. S. & Zohner, C. M. Climate change and phenological mismatch in trophic interactions among plants, insects, and vertebrates. *Annu. Rev. Ecol. Evol. Syst.* **49**, 165–182 (2018).

41. Miller-Rushing, A. J., Høye, T. T., Inouye, D. W. & Post, E. The effects of phenological mismatches on demography. *Philos. Trans. R. Soc. B: Biol. Sci.* **365**, 3177–3186 (2010).

42. McKinney, M. L. Effects of urbanization on species richness: a review of plants and animals. *Urban Ecosyst.* **11**, 161–176 (2008).

43. Walker, J. S., Grimm, N. B., Briggs, J. M., Gries, C. & Dugan, L. Effects of urbanization on plant species diversity in central Arizona. *Front. Ecol. Environ.* **7**, 465–470 (2009).

44. United Nations Environment Programme. *Noise, Blazes and Mismatches*. (Emerging Issues of Environmental Concern. Nairobi, 2022).

45. Heberling, J. M., Miller, J. T., Noesgaard, D., Weingart, S. B. & Schigel, D. Data integration enables global biodiversity synthesis. *Proc. Natl Acad. Sci.* **118**, e2018093118 (2021).

46. Gonzalez, A. et al. A global biodiversity observing system to unite monitoring and guide action. *Nat. Ecol. Evol.* **7**, 1947–1952 (2023).

47. Zhang, J. & Qian, H. U. Taxonstand: An R package for standardizing scientific names of plants and animals. *Plant Diversity* **45**, 1–5 (2023).

48. Zhang, T. et al. A global dataset of daily near-surface air temperature at 1-km resolution. *Earth Syst. Sci. Data* **14**, 5637–5649 (2022).

49. Karger, D. N. et al. Climatologies at high resolution for the earth's land surface areas. *Sci. Data* **4**, 170122 (2017).

50. Amatulli, G. et al. A suite of global, cross-scale topographic variables for environmental and biodiversity modeling. *Sci. Data* **5**, 180040 (2018).

51. Center for International Earth Science Information Network - CIESIN - Columbia University. *Gridded Population of the World, Version 4 (GPWv4): Population Density Adjusted to Match 2015 Revision UN WPP Country Totals, Revision 11.* (NASA Socioeconomic Data and Applications Center (SEDAC), Palisades, New York, 2018).

52. Dixon, P. VEGAN, a package of R functions for community ecology. *J. Vegetation Sci.* **14**, 927–930 (2003).

53. Fu, Y. H. et al. Three times greater weight of daytime than of nighttime temperature on leaf unfolding phenology in temperate trees. *N. Phytol.* **212**, 590–597 (2016).

54. Zhang, Y. et al. The divergent response of vegetation phenology to urbanization: a case study of Beijing city, China. *Sci. Total Environ.* **803**, 150079 (2022).

55. Liang, L., Schwartz, M. D. & Fei, S. Validating satellite phenology through intensive ground observation and landscape scaling in a mixed seasonal forest. *Remote Sens. Environ.* **115**, 143–157 (2011).

56. Huete, A. et al. Overview of the radiometric and biophysical performance of the MODIS vegetation indices. *Remote Sens. Environ.* **83**, 195–213 (2002).

57. Li, X. et al. A dataset of 30 m annual vegetation phenology indicators (1985–2015) in urban areas of the conterminous United States. *Earth Syst. Sci. Data* **11**, 881–894 (2019).

58. Zhu, Z. & Woodcock, C. E. Object-based cloud and cloud shadow detection in Landsat imagery. *Remote Sens. Environ.* **118**, 83–94 (2012).

59. Zohner, C. M., Benito, B. M., Svenning, J.-C. & Renner, S. S. Day length unlikely to constrain climate-driven shifts in leaf-out times of northern woody plants. *Nat. Clim. Change* **6**, 1120–1123 (2016).

60. Vitasse, Y. Ontogenic changes rather than difference in temperature cause understory trees to leaf out earlier. *N. Phytol.* **198**, 149–155 (2013).

61. Wu, Z. Source data for "Tree species composition governs urban phenological responses to warming". Zenodo. https://doi.org/10.5281/zenodo.14864842 (2025).

62. Wu, Z. Code for "Tree species composition governs urban phenological responses to warming". Zenodo. https://doi.org/10.5281/zenodo.15025737 (2025).

Acknowledgements

Author contributions

Y.H.F. conceived the study; Y.H.F., Z.W., and C.M.Z. developed the methodology and analyses; Z.W. conducted the experiment and the corresponding analysis; Y.G. assisted with the experiment. Y.Y.Z. and Y.W. provided the satellite-based phenological datasets; Y.W., Y.B.Z. and J.V.H. contributed to the data preparation; H.W. helped with the analysis of cities in the Northern Hemisphere; Z.W., C.M.Z. and Y.H.F. led the writing of the manuscript in cooperation with Y.Y.Z., T.W.C., J.P., and J.Z.; All authors discussed the methods and results, and contributed critically to the drafts and gave final approval for publication. Z.W. and C.M.Z. contributed equally to this study.

Competing interests

The authors declare no conflict of interests.

Additional information

Supplementary information The online version contains supplementary material available at
https://doi.org/10.1038/s41467-025-58927-8.

Correspondence and requests for materials should be addressed to Yongshuo H. Fu.

Peer review information *Nature Communications* thanks the anonymous reviewers for their contribution to the peer review of this work. A peer review file is available.

Reprints and permissions information is available at http://www.nature.com/reprints

Publisher's note Springer Nature remains neutral with regard to jurisdictional claims in published maps and institutional affiliations.